

See discussions, stats, and author profiles for this publication at: <https://www.researchgate.net/publication/51717215>

NSAID-Based gamma-Secretase Modulators Do Not Bind to the Amyloid-beta Polypeptide

ARTICLE *in* BIOCHEMISTRY · NOVEMBER 2011

Impact Factor: 3.02 · DOI: 10.1021/bi201371j · Source: PubMed

CITATIONS

20

READS

25

5 AUTHORS, INCLUDING:



Paul Barrett

Vanderbilt University

13 PUBLICATIONS 283 CITATIONS

[SEE PROFILE](#)



Klaus Michelsen

Amgen

17 PUBLICATIONS 382 CITATIONS

[SEE PROFILE](#)



John Brad Jordan

Amgen

15 PUBLICATIONS 357 CITATIONS

[SEE PROFILE](#)

Published in final edited form as:

Biochemistry. 2011 November 29; 50(47): 10328–10342. doi:10.1021/bi201371j.

NSAID-Based γ -Secretase Modulators Do Not Bind to The Amyloid- β Polypeptide[†]

Paul J. Barrett[‡], Charles R. Sanders[‡], Stephen A. Kaufman[#], Klaus Michelsen[§], and John B. Jordan^{*,§}

Dept. of Biochemistry and Center for Structural Biology, Vanderbilt University, Nashville, Tennessee 37232-8725, and Dept. of Molecular Structure and Dept. of Pathology, Amgen Inc., Thousand Oaks, California, 91320

Abstract

Gamma secretase modulators (GSMs) have received much attention as potential therapeutic agents for Alzheimer's disease (AD). GSMs increase the ratio between short and long forms of the amyloid- β (A β) polypeptides produced by gamma-secretase and thereby decrease the amount of the toxic amyloid species. However, the mechanism of action of these agents is still poorly understood. One recent paper (Richter et al., *PNAS* **107**, 14597–14602 2010) presented data that were interpreted to support direct binding of the GSM sulindac sulfide to A β ₄₂, supporting the notion that GSM action is linked to direct binding of these compounds to the A β domain of its immediate precursor, the 99 residue C-terminal domain of the amyloid precursor protein (C99, also known as the β -CTF). Here, contrasting results are presented that indicate there is no interaction between monomeric sulindac sulfide and monomeric forms of A β ₄₂. Instead, it was observed that sulindac sulfide is itself prone to form aggregates that can bind non-specifically to A β ₄₂ and trigger its aggregation. This observation, combined with data from previous work (Beel et al., *Biochemistry* **48**, 11837–11839), suggests both that the poor behavior of some NSAID-based GSMs in solution may obscure results of binding assays and that NSAID-based GSMs do not function by directly targeting C99. It was also observed that another GSM, flurbiprofen, fails to bind to monomeric A β ₄₂ or to C99 reconstituted into bilayered lipid vesicles. These results disfavor the hypothesis that these NSAID-based GSMs exert their modulatory effect by directly targeting a site located in the A β ₄₂ domain of free C99.

Alzheimer's disease (AD) is one of the most common neurodegenerative disorders, affecting more than 26 million people worldwide - a number that is expected to more than quadruple by the year 2050(1). AD is characterized by cognitive decline induced by a loss of neurons and synapses in the cerebral cortex (2). This degeneration of neural activity is associated with the existence of extracellular amyloid plaques and intracellular neurofibrillary tangles, both of which characterize the pathology of the disease (3). The neural plaques are comprised of insoluble deposits of amyloid- β (A β) peptides, which result from sequential proteolytic cleavage reactions of the amyloid precursor protein (APP) involving β - and γ -secretase. The APP substrate is first cleaved by β -secretase (BACE-1) to release its large

[†]This work was supported by NIH grant PO1 GM080513 (to CRS) and by Alzheimer's Association grant IIRG-07-59379 (to CRS). Partial support for PB was through NIH T32 NIH 5 T32 GM08320.

^{*}To whom correspondence should be addressed. brad.jordan@amgen.com ; Phone: 805- 313-5647; Fax: 805-498-9057.

[‡]Dept. of Biochemistry and Center for Structural Biology, Vanderbilt University

[§]Dept. of Molecular Structure, Amgen Inc.

[#]Dept. of Pathology, Amgen, Inc.

SUPPORTING INFORMATION AVAILABLE

Eight figures containing further details of the NMR and SPR characterization of the peptides and small molecules used in this study. This material is available free of charge via the Internet at <http://pubs.acs.org>.

ectodomain from a 99 residue transmembrane bound C-terminal fragment (C99, also referred to as β -CTF). C99 then serves as a substrate for γ -secretase, cleavage by which results in release of the APP intracellular domain (AICD) and the A β polypeptide. The A β produced is not completely homogeneous, but varies in length, with A β 42 and A β 40 being the most prominent products. A β 42 is believed to be the most neurotoxic of the amyloid- β polypeptides due to its particularly high propensity to form toxic aggregates that go on to form the amyloid plaques that are the hallmark of AD pathology.

The well defined pathology of AD, first described in the mid-1980s (4–7), set the stage for the proposal of the “amyloid hypothesis” by John Hardy (8), which postulates that accumulation of A β in the brain is the primary cause of AD pathology. The amyloid hypothesis is strongly supported by the observation that all mutations of APP or the Presenilin component of γ -secretase observed in early onset Alzheimer’s disease (EOAD) or familial Alzheimer’s disease (FAD) result either in an increase in total A β levels or in elevated production of A β 42 relative to A β 40 –thus supporting the relationship between the production of A β 42 and the clinical symptoms of AD(2, 8, 9).

To date, there are only five FDA approved treatments for AD in the United States, all of which treat cognitive decline and symptoms of the disease(2). Therefore, the development of a disease-modifying agent – one that prevents or reverses the pathology of the disease — represents a significant unmet medical need. Two promising targets from a drug discovery perspective are β - and γ -secretase. The development of potential therapeutics targeting these two proteins has been extensively reviewed(10–12). Among the proposed strategies, development of agents that *modulate* A β production has recently received much attention. A γ -secretase modulator (GSM) is defined as a molecule that changes the relative proportions of the A β isoforms produced by γ -secretase (particularly A β 42 vs. the less toxic A β 40), without altering the overall rate of APP processing(2). The first GSMs originated from non-steroidal anti-inflammatory drugs (NSAIDs), which were reported to reduce the occurrence of AD in patients using these drugs (13–15). The early NSAIDs, including sulindac sulfide, flurbiprofen, and ibuprofen, were shown to reduce the levels of the highly amyloidogenic A β 42(13, 16, 17). Recent photoaffinity-cross-linking experiments led to the proposal that GSMs bind directly to the transmembrane APP/C99 substrate (18) to form a complex that somehow then modulates γ -secretase cleavage. The site of GSM binding within C99 was proposed to be located in its N-terminal A β 42 domain. However, recent NMR studies from our labs failed to reveal any binding of the GSMs flurbiprofen and fenofibrate to monomeric or dimeric C99 in micellar model membranes, with the binding being detectable only to C99 *aggregates*, which was found to be of a non-specific and non-stoichiometric nature(19). More recently, Multhaup et al. have countered our findings based on NMR, SPR, and bacterial reporter assay results that they interpreted as providing proof that the NSAID-based GSM sulindac sulfide binds avidly and specifically to both A β 42 and C99(20, 21).

We hypothesize that alternative interpretations are merited for some of the key results from Multhaup and co-workers, and also that some of the experiments of those works may have had unrecognized artifacts. Here, we provide additional data to both clarify the previously published data and to provide new data informing on this controversy. The results support our earlier contention(19) that monomeric GSMs either do not bind monomeric or dimeric forms of C99 or A β 42 at all (in solution, in micelles, or in membranes) or bind in a weak and non-specific manner that is likely to be unrelated to their GSM activity. Moreover, these studies revealed that sulindac sulfide forms colloid-like assemblies at concentrations above 50 μ M, a phenomenon that may have been a source of experimental artifacts in some previous studies of GSMs.

Materials and Methods

Reagents, Peptides, and Proteins

A β 40 and A β 42 peptides in both isotopically unlabeled and uniformly-¹⁵N labeled forms were obtained from rPeptide, LLC (Bogart, GA). For all experiments, peptides were first “monomerized” as previously described (22, 23) by dissolving lyophilized material in 98% formic acid and then immediately evaporating the solvent. This “monomerized” material was stored at –20°C and thawed immediately before use. The compounds used in this study, sulindac sulfide, sulindac sulfone, and flurbiprofen, were obtained from Toronto Research Chemicals (North York, ON, CA), MP Biomedicals (Solon, OH), and Sigma-Aldrich (St. Louis, MO).

C99 was recombinantly expressed as described by Beel et al(19). The mammalian C99 vector was cloned into a pET-21a vector and then transformed into the BL21(DE3) *E. coli* strain. Protein overexpression was induced via the addition of isopropyl thiogalactoside to 1mM when cells reached an optical density of approximately 0.8. Cells were harvested and lysed, resulting in C99 localization to inclusion bodies. The inclusion bodies were solubilized using a 0.2% SDS/8M urea buffer. C99 was purified via IMAC, during which SDS and urea were removed and replaced with 0.05% LMPG, a lyso-phospholipid detergent. C99 was eluted from the IMAC column using a buffer containing 250mM imidazole and 0.05% LMPG at pH 7.8. For all experiments performed on C99 in LMPG micelles, the final buffer concentration was 100mM imidazole, 10% LMPG, and 2mM EDTA at pH 6.5.

Sample Preparation

All A β 40 and A β 42 samples were prepared by dissolving the “monomerized” polypeptide in 20mM NaOH at a concentration of 1mg/ml. The resulting solution was the diluted with sample buffer (50mM sodium phosphate, pH 7.0, 10% D₂O) to the desired concentrations, typically 100 μ M.

C99 reconstitution into lipid vesicles began with protein purification as described above, with the only difference being that the final elution buffer consisted of 0.2% SDS in lieu of 0.05% LMPG. Purified C99 in SDS was concentrated using centrifugal ultrafiltration to a final concentration of 1mM. The concentrated C99 solution was then mixed with a SDS/lipid mixture of 400mM SDS/75mM POPC/25mM POPG (400mM SDS:100mM lipid), resulting in a clear solution. The C99/SDS/lipid mixture was then subjected to extensive dialysis to remove all SDS present, during which process C99/POPC/POPG vesicles spontaneously formed. The 4L dialysis buffer (50mM imidazole and 2.25mM EDTA at pH 6.5) was changed three times daily. Completion of dialysis was determined when the C99/lipid solution became cloudy and the surface tension of the dialysate indicated complete removal of detergent. The C99/lipid vesicles solution was then extruded using a 50nm filter to generate unilamellar vesicles, concentrated to a 1mM:100mM C99:lipid ratio, and flash frozen for later experiments. For the NMR studies (GSM titrations), the solution was diluted with buffer to achieve 100 μ M C99 plus 10mM lipid. For vesicle-only control samples, the same dialysis procedure was carried out in parallel, minus C99.

CD Spectroscopy

Far-UV CD spectra were obtained on an AppliedPhotophysics Chirascan spectropolarimeter at ambient temperature. The peptides were analyzed at a concentration of 0.5-1mg/ml, using a quartz cuvette with a pathlength of 0.02 cm (far UV CD, 180–250 nm); the spectra were corrected for contributions from the buffer. Each spectrum represents an average of 3 scans.

Dynamic Light Scattering

DLS experiments were conducted on a DynaPro Plate Reader WPR-06 (Wyatt Technology Corporation, Santa Barbara, CA) using a laser wavelength of 832.4nm. Briefly, 100 μ L volumes of solutions of Triton X-100, sulindac sulfide, sulindac sulfone, and flurbiprofen were prepared (from 50mM DMSO stocks) at concentrations of 5, 10, 25, 50, 100, 200, 300, 400, 600, 800, and 1000 μ M. All solutions were prepared so that the final DMSO concentration was constant at 2% in all samples. Triton X-100 was used as a positive control, and the intensity of the scattered light was measured as a function of drug concentration (Fig 2). All experiments were performed in triplicate at 15°C. Ten acquisitions were performed (10s acquisition time) for each concentration point. Data were processed using the Dynamics 6.10.0.10 software (Wyatt Technology Corporation, Santa Barbara, CA). The average laser light scattering from three experiments were plotted versus concentration to obtain the critical micelle concentration (CMC) or “critical aggregate concentration”, (CAC). The CMC of Triton X-100 was determined to be approximately 200–300 μ M, a value consistent with that in the literature (24).

NMR Spectroscopy

NMR experiments were performed on Bruker Avance II 500MHz and Avance III 800 MHz NMR spectrometers, both equipped with TCI cryoprobes. ^{19}F NMR measurements were performed on the Avance II 500 MHz system using an SEF cryoprobe. All experiments using the amyloid peptides were performed at 5°C. Relaxation and diffusion measurements were used to verify the oligomeric state of the A β peptides used in this study. It is well known that A β 40 has a lower propensity to form large oligomeric fibril species (25). Thus, this peptide was used to compare the behavior of the A β 42 species in solution. For ^{15}N relaxation measurements, NMR experiments were performed at 500 MHz. T_1 and T_2 values were measured as described in Kay et al (26). T_1 and T_2 values for A β 40 and A β 42 were determined from measurements performed on the 500 MHz system using 100 μ M solutions of A β 40 and A β 42. Peak intensities were measured by integration of the region between 7.5–8.8 ppm. T_1 measurements were made using delays of 2, 20, 50, 100, 200, 300, 400, 600, 800, 1000, and 1200 ms. T_2 measurements were made using delays of 0, 16, 32, 48, 64, 80, 96, 128, 160, 192, and 240 ms. The intensities were fit to a single exponential function ($I(t) = I_0 e^{-t/T_2}$) using the program GraphPad Prism (GraphPad Software, La Jolla, CA). T_1 and T_2 values for both A β 40 and A β 42 were estimated to be approximately 620ms and 150ms, respectively. The resulting correlation time (τ_c) for both molecules was then calculated using the following equation (27):

$$\tau_c = \frac{\sqrt{\frac{6T_1}{T_2}} - 7}{4\pi\nu_n} \quad (1)$$

where T_1 and T_2 are the respective relaxation times and ν_n is the spectrometer frequency in Hertz. The resulting calculations yielded correlation times of 3.9 ns for both A β 40 and A β 42 which, at 5°C and taking into account the viscosity of water at this temperature (approximately 1.5x that at ambient), corresponds to a protein of approximately 4.9 kDa – a value consistent with the rotational correlation time for a 4.2 kDa protein (as calculated from the Stokes-Einstein equation) (28).

To further classify the oligomeric state of the peptides in solution, pulsed field gradient diffusion measurements were performed at 500 MHz using a stimulated echo experiment (29). Using dioxane in the solution as a reference (as in (30)), solutions of A β 40 and A β 42 (both 100 μ M) were measured with diffusion gradient strengths varying between 1% and 90% of maximum value. The lengths of the diffusion gradient and stimulated echo were

optimized to give a total decay in the protein signal of ~80%. The spectra were acquired with 32K complex points and a spectral window of approximately 6500 Hz. Data was processed using Topspin 2.1 (Bruker Biospin, Billerica, MA). To obtain diffusion decay rates, the dioxane peak and the methyl region of the spectra (0.3-0.7ppm) were integrated at each data point and fit to equation (2) to determine the decay rate:

$$s(g) = Ae^{-dg^2} \quad (2)$$

where the intensities of the protein signals s are plotted as a function of gradient strength, g , to enable determination of the decay rate, d . Decay rates were determined to be $1.6 \times 10^{-4} \text{ s}^{-1}$ for both peptides. The hydrodynamic radii for A β 40 and A β 42 were then calculated as in Wilkins et al (30) to both be approximately 16Å, which as in Wilkins et al. correspond to a polypeptide chain of approximately 42 residues (30). Using this hydrodynamic radius and the viscosity of water at 5 degrees Celsius, the diffusion coefficient, D , was calculated using the Stokes-Einstein relationship:

$$D = \frac{K_B T}{6\pi\eta r} \quad (3)$$

Where K_B is the Boltzmann constant, T is temperature (K), η is solvent viscosity in kg/m.s at 5°C, and r is the hydrodynamic radius in meters.

Titration of ^{15}N -labeled A β 40 and A β 42 were performed using an 800 MHz NMR spectrometer at 5°C with 100 μM protein solutions. Titrations were performed with sulindac sulfide, sulindac sulfone, flurbiprofen, and DMSO (as a control) and were carried out in two modes. First, 50mM ligand stocks were prepared in DMSO- d_6 . Sulindac sulfide and sulindac sulfone were added to 100 μM protein solutions at concentrations of 5, 10, 50, 100, 300, and 500 μM . Flurbiprofen was added at concentrations of 500 μM and 1mM. Control DMSO-only titrations were performed for each series using the final titration point, which contained 2% DMSO by volume. In addition, titrations with sulindac sulfide, sulindac sulfone, and DMSO were performed as in Richter et al (20), where one titration data point was acquired using 100 μM A β 42 and either 300 μM sulindac sulfide, 300 μM sulindac sulfone, or DMSO-only control. In each case a fresh peptide sample was prepared, the appropriate amount of compound was added (from 50mM DMSO- d_6 stock), and spectra were acquired immediately at 5°C. Time course spectra were acquired at $t=0$, 1hr, and 24hr. When it became evident that the sulindac sulfide was causing aggregation of A β 42, a separate time course experiment was carried out using identical solutions at $t=0$, 15min, and 1hr. All two-dimensional ^{15}N -HSQC spectra were acquired using spectral widths of 12,820 Hz and 2432 Hz in the direct and indirect dimensions, respectively. Data were acquired using 1024 X 64 complex data points and 8 scans per increment. Two-dimensional experiments were also accompanied by 1D proton NMR spectra so that the concentrations of the compounds could be monitored throughout the titration (data not shown).

NMR solubility measurements of sulindac sulfide, sulindac sulfone, and flurbiprofen were performed using a 500 MHz NMR spectrometer in experimental buffer (50mM sodium phosphate, pH 7.0, 10% D_2O) with 2% DMSO- d_6 . Briefly, 50mM stock solutions of each compound were prepared in DMSO- d_6 . For each compound, a 1mM solution was prepared in buffer. Quickly, serial dilutions were made to a final concentration of 5 μM , while keeping the DMSO concentration constant at 2%. 1D proton spectra were measured for each concentration using identical parameters.

To test whether colloidal aggregates of sulindac sulfide can act as promiscuous enzyme inhibitors, β -secretase activity assays were performed in the presence and absence of sulindac sulfide and sulindac sulfone. An NMR-based enzymatic assay was designed using a ^{19}F -labeled BACE-1 substrate peptide — EVNLDAEF(CF₃) — where the trifluoromethyl group is at the meta position on the benzyl ring of Phe. BACE-1 cleaves this peptide between the L and D residues, which results in distinct ^{19}F NMR signals for the substrate and product. The assay was conducted in a 96 well plate format, where each well contained 220nM of CHO-expressed BACE-1 prepared in 20mM sodium acetate buffer, pH 5.0, to which were added sulindac sulfide and sulindac sulfone at various concentrations (3.15, 6.25, 12.5, 25, 50, 100, and 200 μM) followed by a blank DMSO control and a positive control using an inhibitor with a known K_i value. The reaction was started by addition of 100 μM substrate peptide prepared from a 100mM DMSO stock in buffer (20mM sodium acetate, pH 5.0). Cleavage was allowed to proceed for a period of 20 minutes, at which time the reaction was quenched by the addition of 300 μL of 8M urea. Samples were then transferred from the 96 well plate to NMR tubes for analysis. ^{19}F NMR spectra showed the presence of both substrate and product, the peak integrals of which were used to calculate the concentration of each species and to assess the degree of inhibition (31).

Surface Plasmon Resonance

SPR experiments were performed using a Biacore S51 instrument and a CM5 sensor chip (GE Healthcare). Monomerized A β 42 peptide (1mg/ml diluted 1:10 with 10mM sodium acetate, pH 3.4) was immobilized to the sensor chip by standard amine coupling (with ~3000 response units (RU)). Compounds were diluted from DMSO stock solutions in three different running buffers (50mM sodium phosphate, 100mM NaCl, pH 7.0, 2% DMSO (0.2% Tween-20, 0.005% Tween-20, and no detergent). Injections were performed for 55s at a flow rate of 30 $\mu\text{L}/\text{min}$ and 25 degrees C. Data were analyzed using the Scrubber software (BioLogic Software, Campbell ACT, Australia) and were plotted using GraphPad Prism (GraphPad Software, La Jolla, CA).

Transmission Electron Microscopy

Samples were prepared for transmission electron microscopy (TEM) in an identical manner to the NMR samples. Briefly, “monomerized” peptide was dissolved in 20mM NaOH at a concentration of 1mg/ml. Solutions for TEM were prepared at 100 μM . Subsequently, sulindac sulfide and sulindac sulfone were added to final concentrations of 300 μM with a DMSO concentration of 2%. Lastly, a drug-free control sample was prepared containing 2% DMSO only. Formvar-coated copper grids were inverted over 50 μL sample droplets for 15 minutes. The grids were then briefly rinsed with one drop of ultrapure water, and the excess water was removed by wicking to the side with blotter paper. Samples were then inverted over drops of 2% aqueous uranyl acetate for 15 minutes and the grids were subsequently washed over three drops of ultrapure water. Following air drying, the grids were examined on a Philips CM120 transmission electron microscope (FEI, Inc., Hillsboro, OR) operated at 80keV. Representative images were captured using a Gatan Model 830 SC200 CCD camera (Gatan, Inc., Pleasanton, CA).

Results

Selection of NSAIDs for Study

The finding that certain NSAIDs decreased the production of A β 42 produced by γ -secretase cleavage led to the observation that these compounds had various effects on the cleavage of APP. For example, compounds such as ibuprofen, fenofibrate, sulindac sulfide, R-flurbiprofen, and indomethacin were shown to decrease the amount of A β 42 produced. Thus, they were considered A β 42-lowering NSAIDs (see reviews in (32, 33)). Other

compounds, such as celecoxib functioned to increase the amount of A β 42 and were thus termed A β 42-increasing NSAIDs. Lastly, several NSAIDs, such as naproxen and sulindac sulfone, were found to have no effect on the production of A β 42. The sulindacs were chosen because these were the primary focus of the recently published studies(20, 21) that closely concern this paper. Sulindac sulfide acts as a GSM while sulindac sulfone has previously been shown to have no GSM-like effect on the production of A β 42 and serves as a negative control. The well- characterized GSM R-flurbiprofen was also chosen for a limited number of experiments. It has a much higher aqueous solubility (up to ca. 1 mM) than sulindac sulfide and may therefore be tested as a representative GSM for experiments that were hindered by the relatively low solubility of sulindac sulfide.

Verification of the Oligomeric State of Amyloid Peptides

We sought to reproduce results that were previously interpreted (20) to indicate that GSMs bind specifically and avidly to monomeric A β 42, results that were previously invoked to support the idea that binding of GSMs to C99 is central to how these compounds modulate amyloid production.

Amyloid peptides, especially A β 42, are known for their propensity to aggregate and form high molecular weight fibrils. For this reason, we first set out to verify the presence of stable, monomeric polypeptide in our samples. Prior to study, the A β 40 and A β 42 peptides were first “monomerized” as previously described (22, 23). CD spectra of A β 42 were obtained to verify that limited or no β -sheet structure existed in resulting solutions (the presence of which would indicate the formation of fibril-like species). Both peptides exhibited predominantly random coil conformations (Fig S1). The oligomeric states of both the A β 40 and A β 42 peptides were then assessed via NMR diffusion measurements. As indicated in Figure 1, the diffusion decay rates of both A β 40 and A β 42 were seen to be identical and correspond to a hydrodynamic radius of approximately 16Å, matching that expected for a ~40 residue peptide (Figure S1) (30). These data also enabled calculation of the absolute diffusion coefficients, D, for both peptides (Fig 1B), which also correspond to expected values for a very small protein in an aqueous solution. In addition, we carried out ¹⁵N NMR relaxation measurements for both A β 40 and A β 42. From these values, a rotational correlation time of 3.9 ns was determined at 5°C (28). This value corresponds to a protein with molecular weight of ~4.9kDa, and confirms that the overwhelming majority of peptides in these samples populated only the monomeric form under the conditions of these experiments (Fig. S2).

Characterization of GSMs

Sulindac sulfide, sulindac sulfone, and flurbiprofen were characterized by dynamic light scattering (DLS) and NMR to determine their solubility and to assess their oligomeric states at the concentrations tested in this and previous work. Using DLS, sulindac sulfide was found to be monomeric below ca. 50 μ M. However, between 50 and 100 μ M, colloidal aggregates of sulindac sulfide clearly form, indicative of a “critical aggregate concentration” for this compound in the 50–100 μ M range (34). At much higher concentrations (starting at 400 μ M) sulindac sulfide begins to precipitate, which is the cause of the non-linear increase in laser light scattering above this concentration (Figure 2). Sulindac sulfone and flurbiprofen were found to be monomeric up to concentrations of 1 mM, as the scattering intensity over the entire range of concentrations of these compounds was found to be the same as buffer alone.

As an orthogonal method for measuring compound solubility, ¹⁹F NMR experiments were performed at concentrations ranging from 5 μ M to 1mM in aqueous buffer and with a fixed concentration of 2% DMSO. From the NMR spectra in Figure S3, it is clear that sulindac

sulfide begins to form colloidal aggregates at some point between 30 and 62 μM as evidenced by the significant broadening and decreasing intensity of the NMR signals at and above 62 μM , demarking the critical aggregation concentration (CAC) of this compound. On the other hand, both sulindac sulfone and flurbiprofen exhibited no significant changes in their NMR spectra (Figs 4–5 and Fig S4 and S5) and appear to remain monodisperse up to concentrations of 1 mM. These NMR data confirm and complement the results of DLS and show that sulindac sulfide forms colloidal (water soluble) aggregates with a CAC in the range of 50–60 μM , whereas sulindac sulfone and flurbiprofen remain monomeric up through 500 μM .

NMR Titrations of A β 42 with GSMs

To determine if NMR spectroscopy demonstrates binding of sulindac sulfide to monomeric A β 42, as claimed in previous work (20) NMR titration experiments were performed with each compound (using 50 mM stock solutions of the drugs in DMSO- d_6). Control titrations were also performed using DMSO only. Figures 3–6 show ^{15}N -HSQC spectra of A β 42 titrated with sulindac sulfide and flurbiprofen (both are NSAIDs and GSMs), sulindac sulfone (a NSAID but not a GSM), and DMSO control. It is clear that the titrations for all three NSAIDs led to only very small spectral changes in the HSQC spectrum of A β 42 (Figures 3A–5A) and that these changes are virtually identical to those observed during the DMSO control titration (Figure 6A). These data provide no evidence for binding of any of the three compounds to monomeric A β 42. However, in the case of sulindac sulfide, 1-D proton NMR spectra showing resonances both from the GSM and from aromatic sides chains of the peptides (Fig. 3B) reveal that the peaks from monomeric A β 42 begin to lose intensity at sulindac sulfide concentrations above 50 μM — concentrations at which we have shown this that GSM begins to form colloidal aggregates. This is confirmed by examining the 1-D ^1H NMR projections of the 2-D TROSY data (Figure 3C). Such changes were not observed for the flurbiprofen, sulindac sulfone, or for the DMSO control (Figures 4B–C, 5B–C, and 6B–C). These data strongly suggest that colloid formation by sulindac sulfide triggers aggregation of A β 42.

In addition to performing an entire titration series with the NSAIDs, experiments were performed as in Richter et al. (20) where a single point was examined at 1:3 protein:ligand concentration (100 μM A β 42 plus 300 μM of either sulindac sulfide, sulindac sulfone, or 2% DMSO control). Upon addition of 300 μM sulindac sulfide, and by the time the sample could be transferred to the spectrometer and the HSQC experiment recorded, some peaks from A β 42 had begun to disappear (Figure 7). This phenomenon was monitored over the next hour. After 15 minutes, nearly all of the A β 42 had aggregated and become NMR-invisible. By 1 hour, none of the ^{15}N -HSQC signals were visible in NMR spectrum. This effect was not observed with sulindac sulfone, flurbiprofen, or DMSO (data not shown). To investigate the whereabouts of the A β 42 peptides, the NMR samples were submitted for transmission electron microscopy (TEM), the results of which are also shown in Fig. 7D–F. Clearly, the addition of sulindac sulfide at concentrations where it forms colloidal aggregates induced the formation of A β 42 fibrils. On the other hand, addition of DMSO (Fig 7F) or of sulindac sulfone (data not shown) had no effect on the oligomeric state of A β 42.

We also looked for direct interaction of three NSAIDs with A β 42 using surface plasmon resonance (SPR). Previously results from Richter et al (20) suggested that sulindac sulfide binds specifically to A β 42. However, upon closer inspection of the SPR data presented in the previous work, it can be observed that binding of sulindac sulfide to immobilized A β 42 was non-saturable over the concentration range tested, suggestive of very weak and/or non-specific binding. To test this hypothesis, we performed SPR experiments in a similar manner as presented in Richter et al. using immobilized A β 42 peptide. For our studies, we also incorporated varying amounts of Tween-20 in the running buffer— zero detergent (as in the

Richter et al.), 0.005% (40 μ M, below its CMC of 60 μ M) and 0.2% (1.6 mM, above CMC) to illuminate whether drug and/or protein aggregation was a factor in the observed SPR response. The results for sulindac sulfone illustrate the patterns expected for the absence of binding (Figure S6). It can be seen that the SPR traces for flurbiprofen (Figure S7), even up to 1 mM, are very similar to those of sulindac sulfone, also indicative of no binding.

In the case of sulindac sulfide (Figure 8), the data is more complex. In the absence of detergent, sulindac sulfide induces a biphasic response suggestive of a rapid binding event followed by a slower second binding event. This second phase is eliminated when the titration is carried out in the presence of a sub-critical micelle concentration (CMC) of detergent, indicating that the slow binding seen in Figure 8A likely represents non-specific association of sulindac sulfide with A β 42 on the sensor chip — association that can be reduced in the presence of another hydrophobic small molecule (i.e. Tween-20 monomers). When the detergent concentration (Tween-20) is raised still higher to >CMC, it is seen that the SPR response (Figure 8C) is comparable to the negative control SPR response observed at similar concentrations of sulindac sulfone. This indicates that the rapid binding event observed in Figs. 8A-B is of colloidal aggregates of sulindac sulfide to A β 42. Sub-micellar concentrations of detergents (as in 8B) do not break up those soluble aggregates, but the presence of detergent micelles (as in 8C) effectively dissolves the aggregates, which is seen to eliminate binding.

Inhibition of β -Secretase by Sulindac Sulfide

The formation of water soluble colloidal drug aggregates is a commonly encountered phenomenon (33, 35–37). Moreover, such aggregates are known to often have very general and non-specific activities as enzyme inhibitors, sometimes being referred to as “promiscuous inhibitors” (35, 38). To provide additional verification of the nature of the aggregates formed by sulindac sulfide at concentrations above 50 μ M we tested to see whether these aggregates have enzyme inhibitory activity. β -secretase (BACE-1) was used as the test enzyme for this experiment. Indeed, we found that sulindac sulfide began to significantly inhibit BACE-1 at concentrations around 50 μ M, with near complete inhibition being approached at 200 μ M (Fig S8). No inhibition was observed with sulindac sulfone (Fig S8, panel B), which we showed above does not form aggregates, at least not below 1 mM. We also found that the level of inhibition with sulindac sulfide was significantly reduced by doubling the BACE-1 concentration from 220nM to 440nM (data not shown). Such acute sensitivity to enzyme concentration is a common trait of aggregation-based inhibitors (33, 35–37, 39), which inhibit enzyme action through a non-specific binding mechanism (39). These colloidal aggregates can bind to proteins with high affinity to envelop the protein, preventing substrate access and thus inhibiting protein function (35, 38). Maintaining a constant compound concentration and doubling the enzyme concentration can allow this effect to be at least partially overcome, resulting in decreased inhibition of the enzyme (35). These combined results indicate that not only do aggregates formed by sulindac sulfide trigger fibrillization of A β 42, but also that these aggregates share properties in common with other “promiscuous inhibitors”.

NMR Titrations of Membrane-Associated C99 with GSMs

In a previous study, we showed that certain GSMs did not bind to C99 monomers and dimers in micellar model membranes (19). Here, we extend this observation to C99 reconstituted into bilayered lipid membranes. Sulindac sulfide, sulindac sulfone, and flurbiprofen each include fluorine atoms, potentiating the use of 19 F NMR to monitor binding. 19 F NMR chemical shifts are exquisitely sensitive to even very minor changes in local environment. C99 was reconstituted into lipid vesicles with a protein to lipid ration of 1:100 (100 μ M C99:10mM POPC/POPG). Vesicles were then titrated with sulindac sulfide,

sulindac sulfone, and R-flurbiprofen. ^{19}F NMR spectra were acquired for each compound in the presence of protein-free vesicles and in the presence of an identical concentration of vesicles containing reconstituted C99 (100 μM).

Unfortunately, no ^{19}F signal could be detected for sulindac sulfide in both the absence and presence of C99, indicating that this compound binds avidly to the vesicles whether the protein is present or not. Vesicles represent a solids-like environment from an NMR standpoint such that a combination of chemical shift anisotropy and ^1H - ^{19}F dipolar coupling lead to extensive linebroadening and disappearance of ^{19}F signals when sulindac sulfide binds to the vesicles. However, the results were more clearly interpretable for an alternative GSM, flurbiprofen, and for the negative control, sulindac sulfone. These compounds yield sharp ^{19}F NMR peaks in the presence of protein-free vesicles (Figure 9), which indicates either that these compounds do not bind to lipid bilayers at all or bind only weakly such that exchange between solution and the membrane is rapid on the NMR time scale, such that the free population predominates. When C99 is also present in the vesicles at a C99-to-drug mole-to-mole ratio of 5:1, it can be seen in Figure 8 that there are no changes in the spectra relative to protein-free conditions: chemical shifts, linewidths, and peak intensities are unchanged by the presence of the protein. This indicates that sulindac sulfone and flurbiprofen do not bind to C99 even when the protein is present at a five-fold molar excess over the 20 μM drug concentration.

Discussion

The subject of substrate-targeting GSMs has been a topic of extensive research and discussion over the past several years. Some results have suggested that NSAID-based GSMs directly target the APP substrate (C99) (18, 20, 21), while others, including our previous work(19), disfavor this interpretation (see review in (32)). In addition to showing that non-aggregated C99 in model membranes does not bind GSMs(19), we also presented data suggesting that C99 was very likely to have been in an aggregated form in critical experiments of the original Kukar et al. studies(18). While GSMs do appear to bind to *aggregated* C99(19), this is unlikely to be relevant to processing of C99 by gamma-secretase *in vivo*. Moreover, the binding was seen to be non-specific in nature.

Our previous work was disputed in a pair of recent papers by the Multhaup lab (20, 21) which presented data that was interpreted as demonstrating that GSMs, sulindac sulfide in particular, specifically recognize and bind to both membrane-associated C99 and the water soluble monomer form of A β 42, the latter of which includes the putative GSM binding site proposed in the original work by Kukar et al.[Kukar, 2008 #589](#). However, we hypothesize that key results and conclusions in the Multhaup papers may have reflected experimental artifacts due to the poor behavior of sulindac sulfide in aqueous solutions. The results of this current work support this hypothesis based on the two primary sets of results, both of which are closely related to the observation that the GSM sulindac sulfide forms colloidal aggregates with a CAC of roughly 50–60 μM . In the first set of results, Richter et al. presented NMR spectra of 100 μM A β 42 before and after addition of 300 μM sulindac sulfide, which showed a profound drug- induced change in the spectrum of the peptide (Figure 3 in(20)). However, a complete titration series was not carried out, which precludes the possible use of this data to support specific and stoichiometric complex formation between the GSM and A β 42. Moreover, the NMR spectrum of A β 42 in the presence of the drug could be interpreted as reflecting the formation of high molecular weight oligomers or aggregates, since many peaks were seen to disappear. The possibility that the GSM might itself be aggregated at 300 μM was not considered, despite the facts that sulindac sulfide is a very hydrophobic compound and that the amyloid- β polypeptides are known to associate non-specifically with small molecule aggregates(33, 37). In the present work, titrations of

monomeric A β 42 by GSMs sulindac sulfide and R-flurbiprofen were followed by NMR spectroscopy, and yielded no evidence for binding of the monomeric drugs to monomeric A β 42. However, it was found that the colloidal aggregates formed by sulindac sulfide at concentrations above 50-60 μ M induced aggregation of A β 42. Based on this result, we believe that the one point titration presented by the Multhaup lab (20) showing dramatic changes in the NMR spectrum of A β 42 upon addition of 300 μ M sulindac sulfide represents the observation of aggregated A β 42 formed in response to the presence of colloidal aggregates of sulindac sulfide.

The second set of results involves our repetition of SPR experiments (see Fig 2 in (20)) in which binding of sulindac sulfide to immobilized A β 42 was tested over a range of drug concentration from 5 to 100 μ M. The SPR experiments described by Multhaup et al. (20) demonstrated a linear dose/response, which precludes the conclusion that a specific complex is forming. In addition, the authors noted in the supplementary information that the apparent K_d varied with concentration and that the stoichiometry of the purported A β 42:Sulindac Sulfide complex varied from 0.2:1 to 2:1. Rather than attributing this to self-association of the compound itself, the authors concluded that the compound bound to multiple binding sites on the A β 42 peptide. Additionally, these experiments were performed under essentially membrane- and micelle-free conditions. (Tween-20 was present during all these steps, but only at 40 μ M, which is below its critical micelle concentration of 60 μ M). This is a problem due to the propensity of these proteins to aggregate in the absence of detergent micelles or some other membrane-mimetic medium. Therefore, the immobilized protein present in the SPR experiments (20, 21) was almost certainly in an aggregated form. We reproduced the observation that sulindac sulfide, but not the negative control sulindac sulfone, induces a strong and dose-dependent SPR response. However, when the sulindac sulfide titration was repeated in the presence of Tween-20 micelles, we observed that there was no SPR response beyond what was observed for negative control conditions. This strongly suggests the binding of sulindac sulfide to A β 42 observed in the earlier work represents *non-specific* association of these two compounds. Such association is highest when sulindac sulfide is in its colloidal form (at concentrations $>50\mu$ M) and may also be promoted by the structural properties of sensor chip surface-associated A β 42, which may itself have aggregate-like properties as a result of being locally concentrated at on the sensor chip surface. Association between the GSM and surface-associated A β 42 is eliminated by the presence of detergent micelles that can disperse the colloidal drug and can also coat exposed hydrophobic sites on sensor surface-associated A β 42, making such sites less-susceptible to non-specific hydrophobic interactions with hydrophobic compounds such as sulindac sulfide. We have previously shown that aggregated C99 can bind GSMs in a non-specific fashion (19) and so it is no surprise that this is what was seen by Multhaup and co-workers(21). In the present work, we observed that the GSM R-flurbiprofen exhibits no binding to C99 reconstituted lipid in vesicles. This result extends the conclusions from our earlier observations of the lack of GSM binding to non-aggregated C99 in *micellar* model membranes to non-aggregated C99 in actual lipid bilayers.

One additional set of experiments from Multhaup and co-workers that yielded support for sulindac sulfide binding to C99 in membranes was a series of ToxR experiments carried out in *E. coli* (20). In those experiments homodimerization of the transmembrane segment of C99 was assessed following expression into *E. coli* based on coupling homodimerization of this segment to transcriptional activation of a gene that expresses a colorimetric reporter enzyme. Using this assay, it was seen that sulindac sulfide reduces apparent dimerization of C99 in *E. coli* in a dose-dependent fashion, consistent with inhibition of dimerization of C99 by GSM binding. These studies were carefully carried out and can indeed be interpreted as being supportive of GSM/C99 binding. However, when conducting *in vitro* experiments involving GSM drugs, living cells, and an indirect phenotype-based assay the possibility

cannot be ruled out that the GSM induces a positive assay response as a result of off-target drug effects that lead to the artifact-based activation of the assay response (i.e., induction of reporter enzyme expression). In light of the biophysical results of this paper, we suggest that this alternative explanation of the ToxR data is very likely applicable.

The experiments and results summarized above lead to the conclusion that the GSM sulindac sulfide does not bind to A β 42 when both compounds are in monomeric form. On the other hand, the results clearly suggest that two types of non-specific binding occur: those between aggregates of A β 42 and monomers of NSAID type compounds (sulindac sulfide, as well as flurbiprofen and celecoxib (19)), and those between colloid-type aggregates of sulindac sulfide and monomeric A β 42. Promiscuous binding of small molecule aggregates to proteins, often accompanied by inhibition of protein function, is a very common occurrence (33, 35–37). Indeed, in this study aggregated sulindac sulfide was found not only to bind to A β 42, but also to inhibit β -secretase (here used as a representative enzyme). It has previously been shown that Congo red can form colloidal micelle-like aggregates that bind to A β and induce its aggregation(37). It has also been observed that a number of drug-like molecules form colloidal aggregates that interact with amyloid-forming yeast prion proteins in a way that inhibits fibril formation(36).

Evidence is accumulating that NSAID-based GSMs do not exert their therapeutic effect by binding to free C99 (review in (32)). Previous publications have suggested that GSMs act by causing conformational changes within Presenilin 1 (PS1)(40–42), or by altering membrane architecture and thereby changing the manner in which γ -secretase cleaves its APP substrate (43). More recent studies have indicated that the action of GSMs may be allosteric in nature. Uemura et al demonstrated that GSM-induced conformational changes in PS1 only occur in the presence of substrate, suggesting that substrate binding to γ -secretase uncovers an allosteric site for GSM binding that is only present in the substrate-enzyme complex (44). Another recent study demonstrated that mutations in the GxxxG motif located in the previously-proposed GSM binding site of C99 still caused an effect on A β 42 production upon treatment with GSMs (45). The compounds were then shown to display differential or no effects on A β 42 and A β 38 levels when PS1 mutants were used, implying disruption of GSM interaction with γ -secretase. These conclusions contradict a free substrate-targeted model of GSM action and instead suggest that these molecules target the γ -secretase enzyme itself or the enzyme-substrate complex (45). The results of this paper rule out binding of GSMs to free C99 in non-aggregated form but do not argue against the possibility that GSMs could interact directly with C99 when is bound to γ -secretase. Taken as a whole, the evidence is becoming overwhelming that GSMs do not specifically target the γ -secretase substrate, at least not prior to its association with the enzyme.

Supplementary Material

Refer to Web version on PubMed Central for supplementary material.

Acknowledgments

This work was supported by NIH grant PO1GM080513 (to CRS) and by Alzheimer's Association grant IIRG-07-59379 (to CRS). Partial support for PB was through NIH T32 GM08320. The authors would like to acknowledge Cynthia Li at Amgen for assistance with CD experiments and Drs. Leszek Poppe, Paul Schnier, and Steve Wood for critical reading of the manuscript.

Abbreviations

APP amyloid precursor protein

β-CTF	99 residue transmembrane C-terminal fragment of the amyloid precursor protein
BACE-1	β-secretase
C99	99 residue transmembrane C-terminal domain of the amyloid precursor protein
NSAID	non-steroidal anti-inflammatory drug
CAC	critical aggregate concentration
CD	circular dichroism
CMC	critical micelle concentration
<i>E. coli</i>	<i>Escherichia coli</i>
GSM	gamma-secretase modulator
MP	membrane protein
NMR	nuclear magnetic resonance
POPC	1-palmitoyl-2-oleoyl-phosphatidylcholine
POPG	1-palmitoyl-2-oleoyl-phosphatidylglycerol
TM	transmembrane
TMD	transmembrane domain
2-D	two-dimensional
UV	ultraviolet

References

1. Brookmeyer R, Johnson E, Ziegler-Graham K, Arrighi HM. Forecasting the global burden of Alzheimer's disease. *Alzheimers Dement*. 2007; 3:186–191. [PubMed: 19595937]
2. Oehlrich D, Berthelot DJ, Gijzen HJ. Gamma-Secretase Modulators as Potential Disease Modifying Anti-Alzheimer's Drugs. *J Med Chem*. 2010
3. Tiraboschi P, Hansen LA, Thal LJ, Corey-Bloom J. The importance of neuritic plaques and tangles to the development and evolution of AD. *Neurology*. 2004; 62:1984–1989. [PubMed: 15184601]
4. Glenner GG, Wong CW. Alzheimer's disease: initial report of the purification and characterization of a novel cerebrovascular amyloid protein. *Biochem Biophys Res Commun*. 1984; 120:885–890. [PubMed: 6375662]
5. Glenner GG, Wong CW, Quaranta V, Eanes ED. The amyloid deposits in Alzheimer's disease: their nature and pathogenesis. *Appl Pathol*. 1984; 2:357–369. [PubMed: 6242724]
6. Masters CL, Multhaup G, Simms G, Pottgiesser J, Martins RN, Beyreuther K. Neuronal origin of a cerebral amyloid: neurofibrillary tangles of Alzheimer's disease contain the same protein as the amyloid of plaque cores and blood vessels. *EMBO J*. 1985; 4:2757–2763. [PubMed: 4065091]
7. Masters CL, Simms G, Weinman NA, Multhaup G, McDonald BL, Beyreuther K. Amyloid plaque core protein in Alzheimer disease and Down syndrome. *Proc Natl Acad Sci U S A*. 1985; 82:4245–4249. [PubMed: 3159021]
8. Hardy JA, Higgins GA. Alzheimer's disease: the amyloid cascade hypothesis. *Science*. 1992; 256:184–185. [PubMed: 1566067]
9. Hardy J, Selkoe DJ. The amyloid hypothesis of Alzheimer's disease: progress and problems on the road to therapeutics. *Science*. 2002; 297:353–356. [PubMed: 12130773]
10. Grill JD, Cummings JL. Current therapeutic targets for the treatment of Alzheimer's disease. *Expert Rev Neurother*. 10:711–728. [PubMed: 20420492]

11. Galimberti D, Scarpini E. Alzheimer's disease: from pathogenesis to disease-modifying approaches. *CNS Neurol Disord Drug Targets*. 10:163–174. [PubMed: 21222635]
12. Aguzzi A, O'Connor T. Protein aggregation diseases: pathogenicity and therapeutic perspectives. *Nat Rev Drug Discov*. 9:237–248. [PubMed: 20190788]
13. Weggen S, Rogers M, Eriksen J. NSAIDs: small molecules for prevention of Alzheimer's disease or precursors for future drug development? *Trends Pharmacol Sci*. 2007; 28:536–543. [PubMed: 17900710]
14. Imbimbo BP. An update on the efficacy of non-steroidal anti-inflammatory drugs in Alzheimer's disease. *Expert Opin Investig Drugs*. 2009; 18:1147–1168.
15. Imbimbo BP. Why did tarenflurbil fail in Alzheimer's disease? *J Alzheimers Dis*. 2009; 17:757–760. [PubMed: 19542625]
16. Weggen S, Eriksen JL, Das P, Sagi SA, Wang R, Pietrzik CU, Findlay KA, Smith TE, Murphy MP, Bulter T, Kang DE, Marquez-Sterling N, Golde TE, Koo EH. A subset of NSAIDs lower amyloidogenic Abeta42 independently of cyclooxygenase activity. *Nature*. 2001; 414:212–216. [PubMed: 11700559]
17. Eriksen JL, Sagi SA, Smith TE, Weggen S, Das P, McLendon DC, Ozols VV, Jessing KW, Zavitz KH, Koo EH, Golde TE. NSAIDs and enantiomers of flurbiprofen target gamma-secretase and lower Abeta 42 in vivo. *J Clin Invest*. 2003; 112:440–449. [PubMed: 12897211]
18. Kukar TL, Ladd TB, Bann MA, Fraering PC, Narlawar R, Maharvi GM, Healy B, Chapman R, Welzel AT, Price RW, Moore B, Rangachari V, Cusack B, Eriksen J, Jansen-West K, Verbeeck C, Yager D, Eckman C, Ye W, Sagi S, Cottrell BA, Torpey J, Rosenberry TL, Fauq A, Wolfe MS, Schmidt B, Walsh DM, Koo EH, Golde TE. Substrate-targeting gamma-secretase modulators. *Nature*. 2008; 453:925–929. [PubMed: 18548070]
19. Beel AJ, Barrett P, Schnier PD, Hitchcock SA, Bagal D, Sanders CR, Jordan JB. Nonspecificity of binding of gamma-secretase modulators to the amyloid precursor protein. *Biochemistry*. 2009; 48:11837–11839. [PubMed: 19928774]
20. Richter L, Munter LM, Ness J, Hildebrand PW, Dasari M, Unterreitmeier S, Bulic B, Beyermann M, Gust R, Reif B, Weggen S, Langosch D, Multhaup G. Amyloid beta 42 peptide (Abeta42)-lowering compounds directly bind to Abeta and interfere with amyloid precursor protein (APP) transmembrane dimerization. *Proc Natl Acad Sci U S A*. 107:14597–14602. [PubMed: 20679249]
21. Botev A, Munter LM, Wenzel R, Richter L, Althoff V, Ismer J, Gerling U, Weise C, Koksche B, Hildebrand PW, Bittl R, Multhaup G. The amyloid precursor protein C-terminal fragment C100 occurs in monomeric and dimeric stable conformations and binds gamma-secretase modulators. *Biochemistry*. 50:828–835. [PubMed: 21186781]
22. Harmeier A, Wozny C, Rost BR, Munter LM, Hua H, Georgiev O, Beyermann M, Hildebrand PW, Weise C, Schaffner W, Schmitz D, Multhaup G. Role of amyloid-beta glycine 33 in oligomerization, toxicity, and neuronal plasticity. *J Neurosci*. 2009; 29:7582–7590. [PubMed: 19515926]
23. Schmechel A, Zentgraf H, Scheuermann S, Fritz G, Pipkorn R, Reed J, Beyreuther K, Bayer TA, Multhaup G. Alzheimer beta-amyloid homodimers facilitate A beta fibrillization and the generation of conformational antibodies. *J Biol Chem*. 2003; 278:35317–35324. [PubMed: 12840025]
24. Ash, M.; Ash, I. *The Handbook of Industrial Surfactants*. Synapse Information Resources, Inc; Endicott, NY: 2010.
25. Roher AE, Chaney MO, Kuo YM, Webster SD, Stine WB, Haverkamp LJ, Woods AS, Cotter RJ, Tuohy JM, Krafft GA, Bonnell BS, Emmerling MR. Morphology and toxicity of Abeta-(1-42) dimer derived from neuritic and vascular amyloid deposits of Alzheimer's disease. *J Biol Chem*. 1996; 271:20631–20635. [PubMed: 8702810]
26. Farrow NA, Muhandiram R, Singer AU, Pascal SM, Kay CM, Gish G, Shoelson SE, Pawson T, Forman-Kay JD, Kay LE. Backbone dynamics of a free and phosphopeptide-complexed Src homology 2 domain studied by 15N NMR relaxation. *Biochemistry*. 1994; 33:5984–6003. [PubMed: 7514039]

27. Kay LE, Torchia DA, Bax A. Backbone dynamics of proteins as studied by ¹⁵N inverse detected heteronuclear NMR spectroscopy: application to staphylococcal nuclease. *Biochemistry*. 1989; 28:8972–8979. [PubMed: 2690953]
28. Cavanagh, J.; Fairbrother, WJ.; Palmer, AG.; Skelton, NJ. *Protein NMR Spectroscopy: Principles and Practice*. Academic Press; San Diego, CA: 1996.
29. Zheng G, Stait-Gardner T, Anil Kumar PG, Torres AM, Price WS. PGSTE-WATERGATE: an STE-based PGSE NMR sequence with excellent solvent suppression. *J Magn Reson*. 2008; 191:159–163. [PubMed: 18086542]
30. Wilkins DK, Grimshaw SB, Receveur V, Dobson CM, Jones JA, Smith LJ. Hydrodynamic radii of native and denatured proteins measured by pulse field gradient NMR techniques. *Biochemistry*. 1999; 38:16424–16431. [PubMed: 10600103]
31. Cheng Y, Judd T, Bartberger M, Chen K, Fremeau R, Hickman D, Hitchcock S, Jordan J, Li V, Lopez P, Louie S, Luo Y, Michelsen K, Nixey T, Powers T, Rattan C, Sickmier E, StJean D, Wahl R, Wen P, Wood S. From Fragment Screening to In Vivo Efficacy: Optimization of a Series of 2-Aminoquinolines as Potent Inhibitors of BACE1. *J Med Chem*. 2011
32. Zettl H, Weggen S, Schneider P, Schneider G. Exploring the chemical space of gamma-secretase modulators. *Trends Pharmacol Sci*. 31:402–410. [PubMed: 20591508]
33. Coan KE, Shoichet BK. Stoichiometry and physical chemistry of promiscuous aggregate-based inhibitors. *J Am Chem Soc*. 2008; 130:9606–9612. [PubMed: 18588298]
34. Feng BY, Shoichet BK. Synergy and antagonism of promiscuous inhibition in multiple-compound mixtures. *J Med Chem*. 2006; 49:2151–2154. [PubMed: 16570910]
35. McGovern SL, Caselli E, Grigorieff N, Shoichet BK. A common mechanism underlying promiscuous inhibitors from virtual and high-throughput screening. *J Med Chem*. 2002; 45:1712–1722. [PubMed: 11931626]
36. Feng BY, Toyama BH, Wille H, Colby DW, Collins SR, May BC, Prusiner SB, Weissman J, Shoichet BK. Small-molecule aggregates inhibit amyloid polymerization. *Nat Chem Biol*. 2008; 4:197–199. [PubMed: 18223646]
37. Lendel C, Bolognesi B, Wahlstrom A, Dobson CM, Graslund A. Detergent-like interaction of Congo red with the amyloid beta peptide. *Biochemistry*. 49:1358–1360. [PubMed: 20070125]
38. McGovern SL, Helfand BT, Feng B, Shoichet BK. A specific mechanism of nonspecific inhibition. *J Med Chem*. 2003; 46:4265–4272. [PubMed: 13678405]
39. Giannetti AM, Koch BD, Browner MF. Surface plasmon resonance based assay for the detection and characterization of promiscuous inhibitors. *J Med Chem*. 2008; 51:574–580. [PubMed: 18181566]
40. Lleo A, Berezovska O, Herl L, Raju S, Deng A, Bacskai BJ, Frosch MP, Irizarry M, Hyman BT. Nonsteroidal anti-inflammatory drugs lower Abeta42 and change presenilin 1 conformation. *Nat Med*. 2004; 10:1065–1066. [PubMed: 15448688]
41. Berezovska O, Lleo A, Herl LD, Frosch MP, Stern EA, Bacskai BJ, Hyman BT. Familial Alzheimer's disease presenilin 1 mutations cause alterations in the conformation of presenilin and interactions with amyloid precursor protein. *J Neurosci*. 2005; 25:3009–3017. [PubMed: 15772361]
42. Uemura K, Lill CM, Li X, Peters JA, Ivanov A, Fan Z, DeStrooper B, Bacskai BJ, Hyman BT, Berezovska O. Allosteric modulation of PS1/gamma-secretase conformation correlates with amyloid beta(42/40) ratio. *PLoS One*. 2009; 4:e7893. [PubMed: 19924286]
43. Gamerding M, Clement AB, Behl C. Effects of sulindac sulfide on the membrane architecture and the activity of gamma-secretase. *Neuropharmacology*. 2008; 54:998–1005. [PubMed: 18359496]
44. Uemura K, Farner KC, Hashimoto T, Nasser-Ghodsi N, Wolfe MS, Koo EH, Hyman BT, Berezovska O. Substrate docking to gamma-secretase allows access of gamma-secretase modulators to an allosteric site. *Nat Commun*. 1:130. [PubMed: 21119643]
45. Page RM, Gutsmedl A, Fukumori A, Winkler E, Haass C, Steiner H. Beta-amyloid precursor protein mutants respond to gamma-secretase modulators. *J Biol Chem*. 285:17798–17810. [PubMed: 20348104]

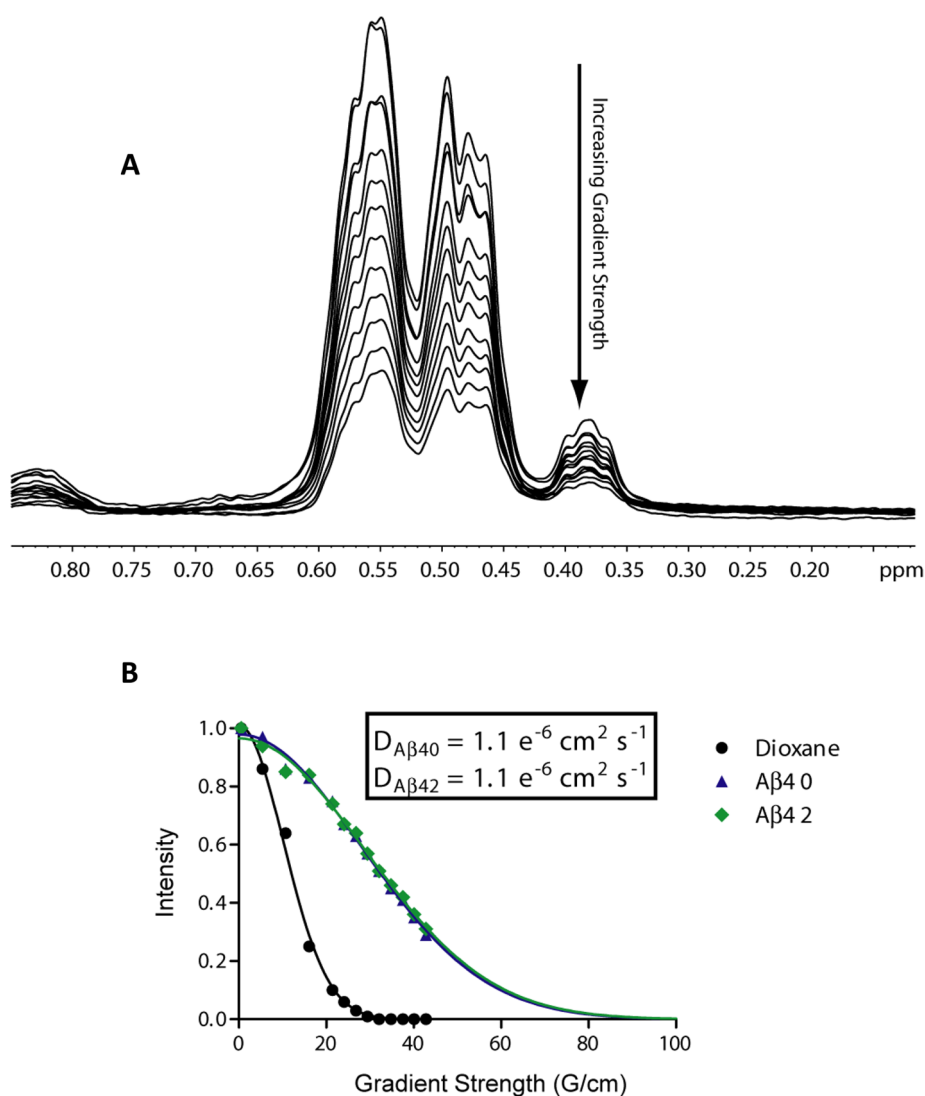


Figure 1.

(A) ¹H NMR-based translational diffusion data for Aβ42 at Z-gradient strengths varying from 0.5 to 42.3 G/cm. The methyl region of the spectrum between 0.7 and 0.3 ppm was integrated for each point to yield relative intensities that were plotted against gradient strength in (B). The intensities in panel A were measured using dioxane as an internal reference and were fit to a single exponential (see Methods) to determine the hydrodynamic radius and diffusion coefficient, *D*, as presented in the inset. Data for the dioxane standard is represented by black circles, Aβ40 by blue triangles, and Aβ42 by green diamonds. Curve fits are represented by solid lines of corresponding colors.

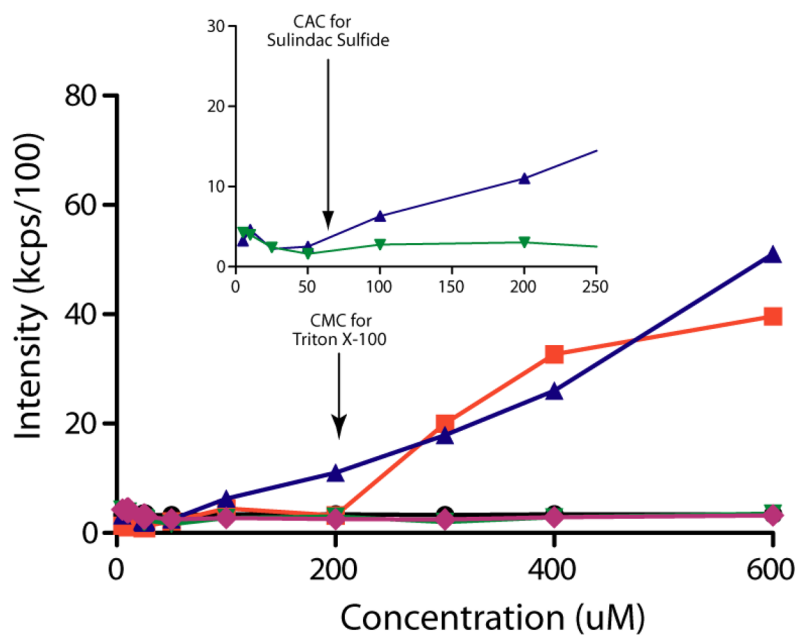
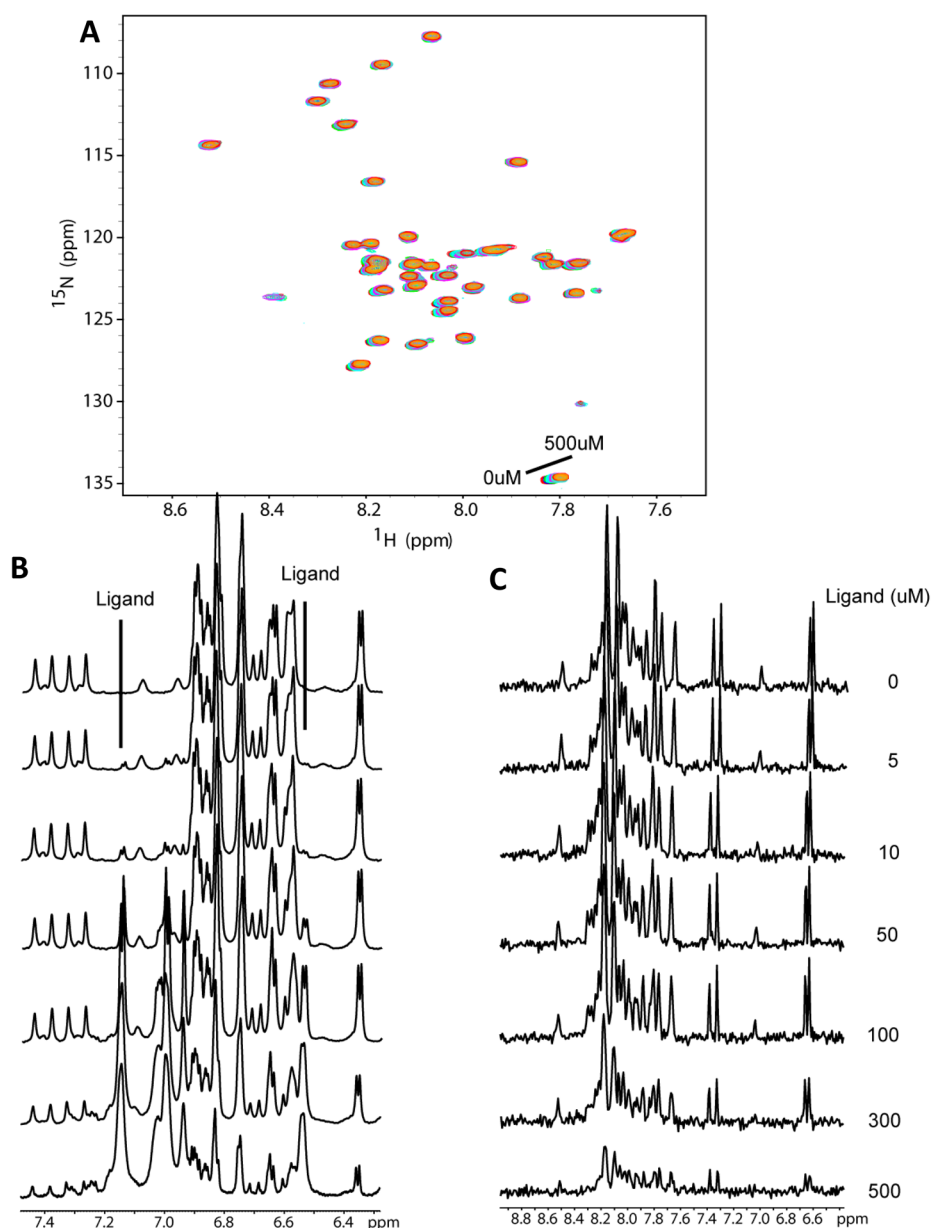
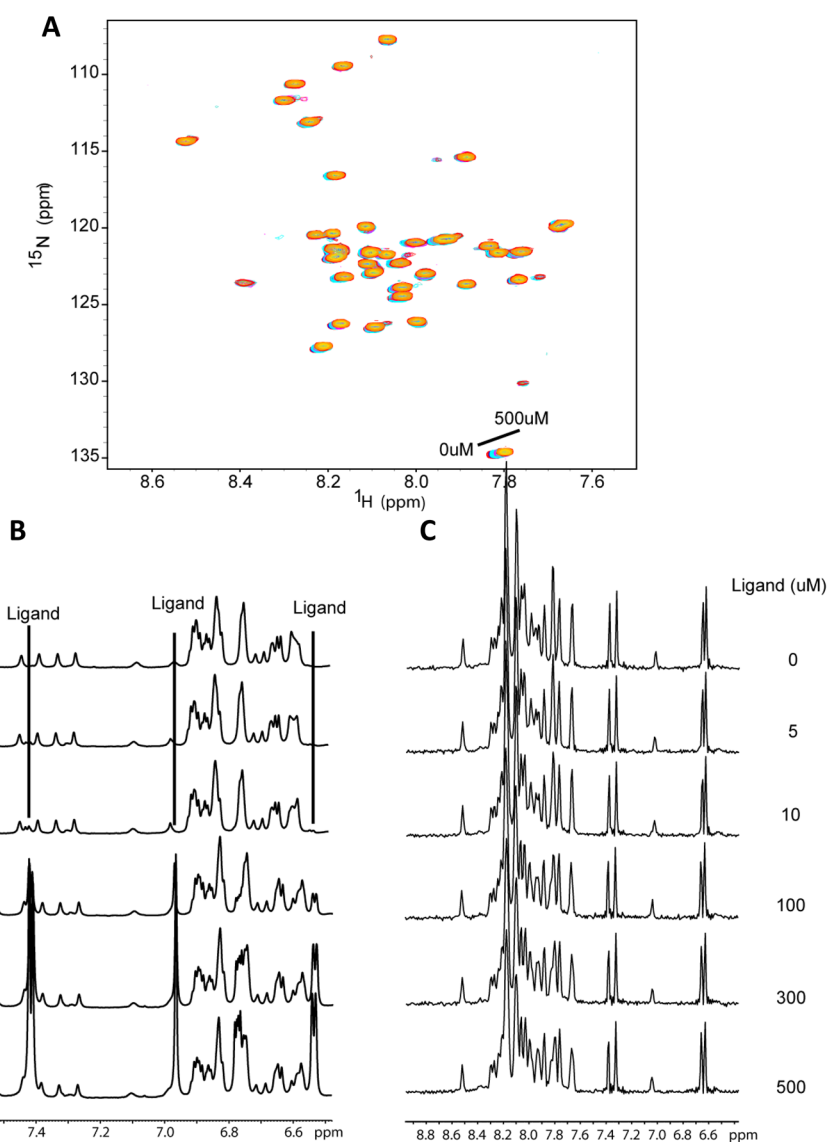


Figure 2.

Measurement of the critical aggregation concentration (CAC) by dynamic light scattering (DLS). Scattering intensities were plotted versus concentration, and the CAC was determined as the point when the scattering intensities began to increase. The legend is as follows: buffer only (black circles), Triton X-100 (orange squares), sulindac sulfide (purple triangles), sulindac sulfone (green triangles), and flurbiprofen (green diamonds). Notice that no increase in scattering intensity was observed for buffer, sulindac sulfone, or flurbiprofen. However, a significant increase in scattering intensity was observed for a positive control (Triton X-100) upon micelle formation at 200-300uM and for sulindac sulfide starting above 50 μ M, indicating that the latter begins to form aggregates at concentrations above 50 μ M, which is consistent with NMR data (Figs S3-S5).

**Figure 3.**

Titration of U- ^{15}N -A β 42 with sulindac sulfide. **(A)** ^{15}N -HSQC spectra of A β 42 upon titration with sulindac sulfide (from a 50mM stock solution in DMSO) at concentrations ranging from 0 to 500 μM . There are no shifts in the peaks of these spectra beyond what is observed for the DMSO-only control titration (see Fig. 6). However, peak intensities decrease at higher sulindac sulfide concentrations. **(B)** ^1H NMR spectra taken at each titration point to allow observation of the ligand peaks throughout the titration. Notice that ligand peaks are observable even at the lowest concentration (5 μM) and with a nearly 20-fold excess of protein, but begin to broaden or disappear above 50-100 μM , indicating aggregation of the compound. **(C)** 1-D ^1H NMR projections of the HSQC spectra shown in panel A illustrate the decrease in amide ^1H signal intensity from the peptide, which demonstrates that A β 42 begins to aggregate upon addition of sulindac sulfide at concentrations above 50 μM .

**Figure 4.**

Titration of U- ^{15}N -A β 42 with sulindac sulfone. **(A)** ^{15}N -HSQC spectra of A β 42 upon titration of sulindac sulfone at concentrations ranging from 0 to 500 μM . There are no shifts in the peaks of these spectra beyond what is observed for the DMSO-only control titration (see Fig. 6) and peak intensities do not vary. **(B)** ^1H NMR spectra taken at each titration point to allow observation of ligand peaks throughout the titration. It can be seen that the sulindac sulfone peaks remain sharp throughout, reflecting the fact that this compound does not aggregate at concentrations below 500 μM . **(C)** 1-D ^1H NMR projections of the HSQC spectra shown in panel A demonstrate that the solubility of A β 42 remains unchanged at all points.

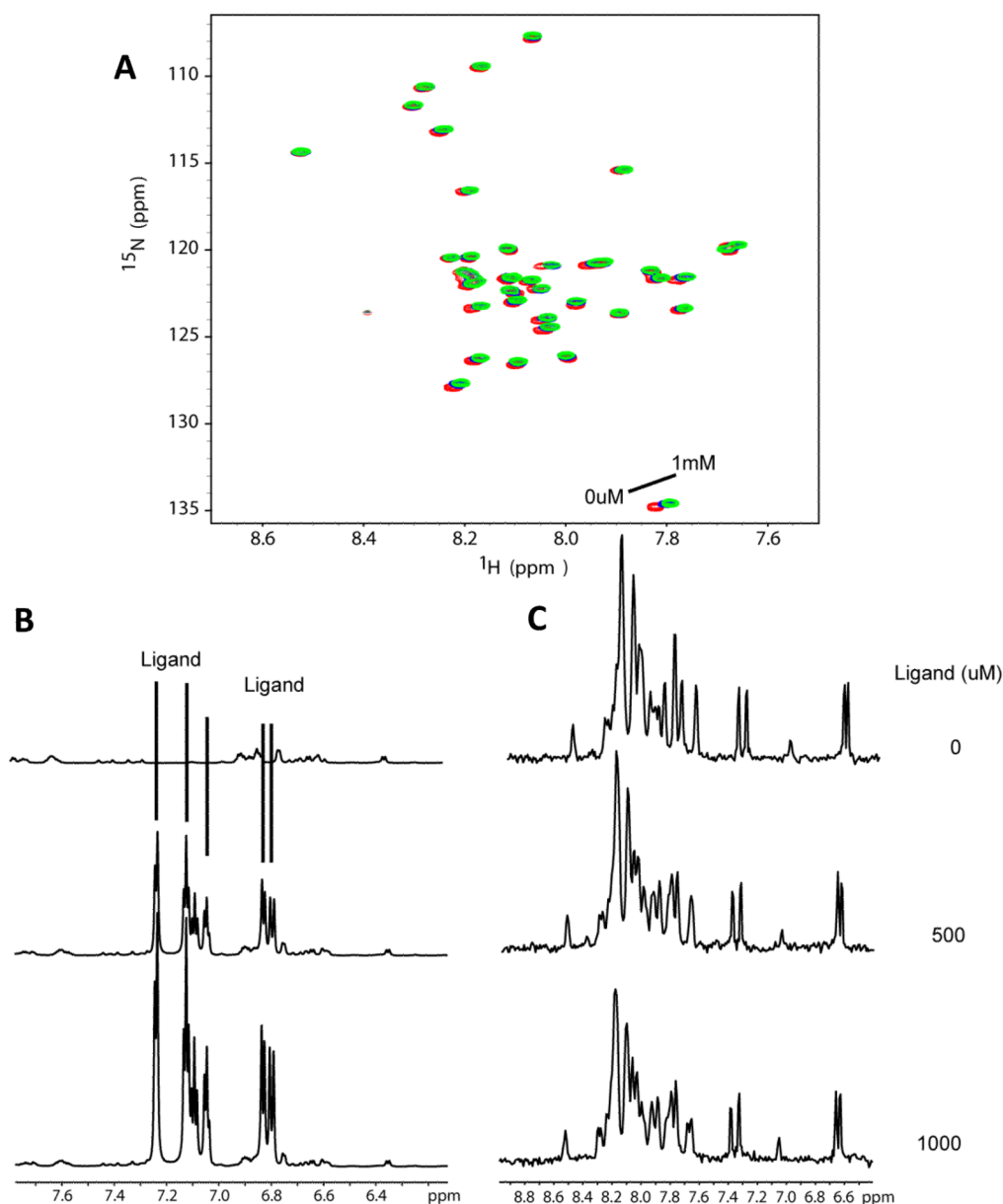


Figure 5.

Titration of U- ^{15}N -A β 42 with flurbiprofen. (A) ^{15}N -HSQC spectra of A β 42 upon titration of flurbiprofen at concentrations of 500uM and 1mM. There are no shifts in the peaks of these spectra beyond what is observed for the DMSO-only control titration (see Fig. 6) and peak intensities do not vary. (B) ^1H NMR spectra taken at each titration point to allow observation of ligand peaks throughout the titration. It can be seen that the flurbiprofen peaks remain sharp throughout, reflecting the fact that this compound does not aggregate at concentrations below 1 mM. (C) 1-D ^1H NMR projections of the HSQC spectra shown in panel A demonstrate that the solubility of A β 42 remains unchanged at all titration points.

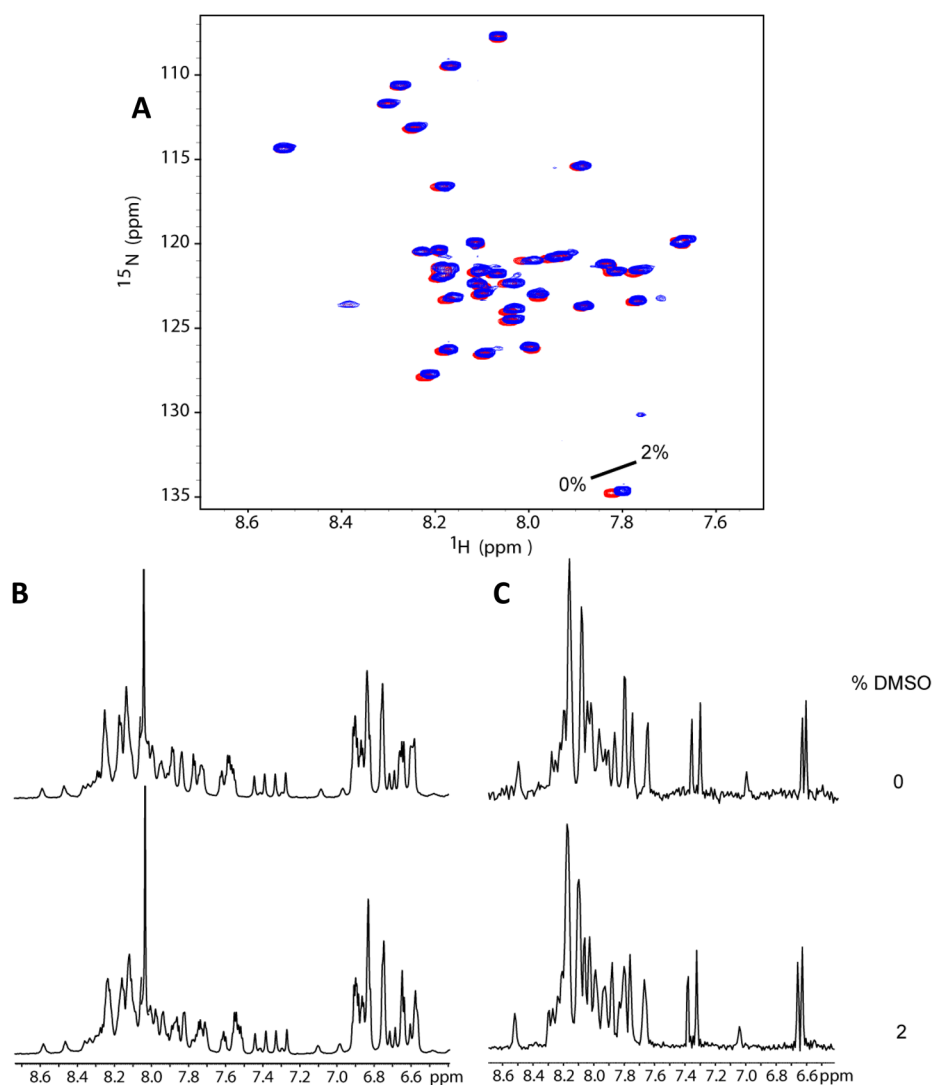


Figure 6.

DMSO control titration spectra of A β 42. (A) ^{15}N HSQC spectra of U- ^{15}N -A β 42 upon addition of DMSO- d_6 at 0% and 2% (initial and final concentrations in titrations of Figs 3–5). (B) 1-D ^1H NMR projections of the HSQC experiments taken in panel A demonstrate that A β 42 remains soluble and monomeric upon addition of DMSO- d_6 to 2%.

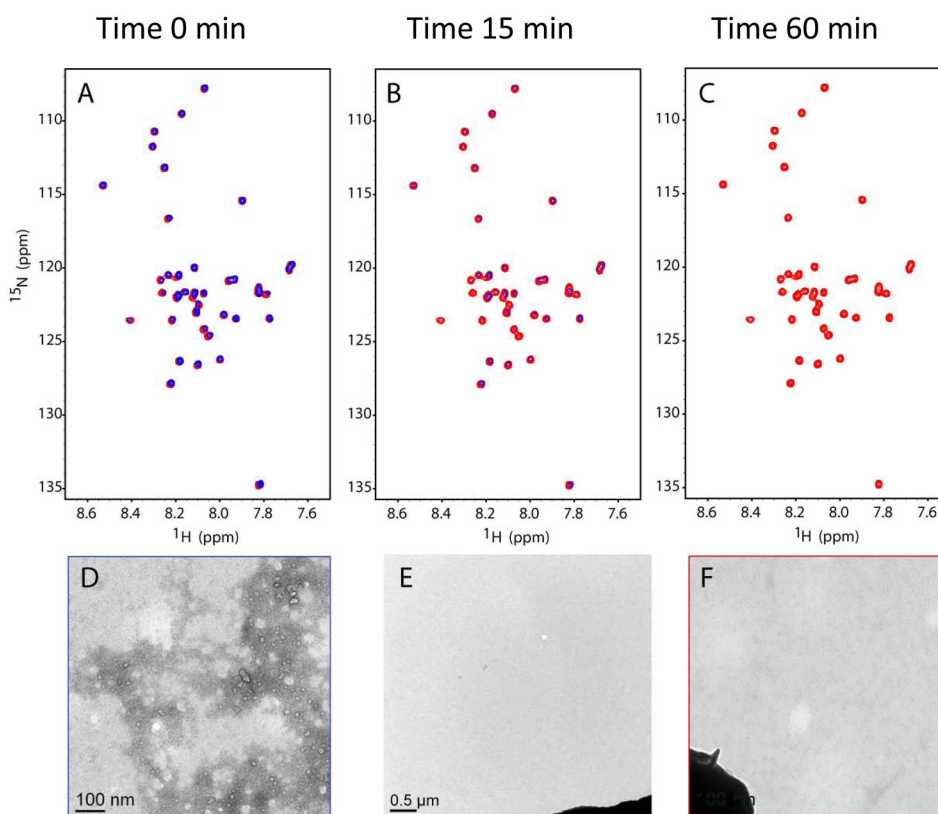


Figure 7.

Time course ^{15}N -HSQC spectra of $100\ \mu\text{M}$ U- ^{15}N -A β 42 following addition of sulindac sulfide to 300 μM . Panels **A**, **B**, and **C** show spectra taken of $100\ \mu\text{M}$ A β 42 alone (red) and upon addition of sulindac sulfide (blue) at times = 0, 15min, and 1hr, respectively. Notice the decrease in intensity of all the blue peaks as A β 42 begins to form aggregates. Panels **D**, **E**, and **F** show transmission electron micrographs (66,000x) of $100\ \mu\text{M}$ A β 42 NMR samples fixed to a TEM grid approximately 2hrs after addition of (**D**) 300 μM sulindac sulfide, (**E**) 300 μM sulindac sulfide alone (no protein, 11,600x), and (**F**) DMSO-only to a final concentration of 2%, matching that in **D** and **E** (dark blob in **E** and **F** is grid bar included for camera gain). In **D**, fibrils of A β 42 are clearly visible.

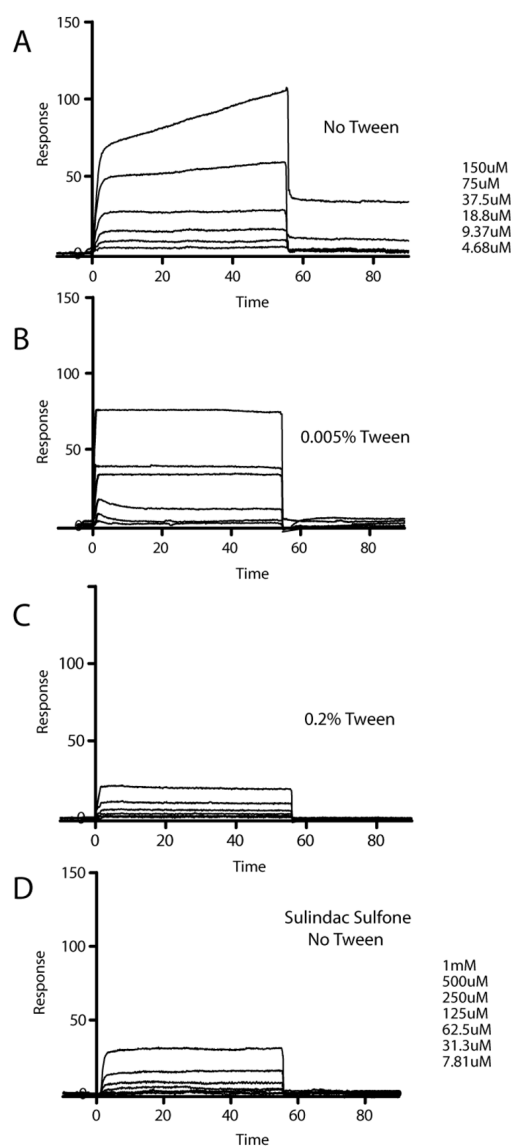


Figure 8.

SPR analysis of sulindac sulfide with immobilized A β 42. Overlays of SPR sensorgrams obtained from injections of sulindac sulfide in 50mM sodium phosphate, 50mM NaCl, pH 7 with (A) No detergent, (B) 0.005% Tween-20, and (C) 0.2% Tween-20. Panel D shows corresponding sensorgrams of sulindac sulfone used as a negative control. A β 42 was immobilized with ~3000 response units (RUs). Compounds at indicated concentration were injected for 55s at a flow rate of 30 μ L/min at 25 degrees C.

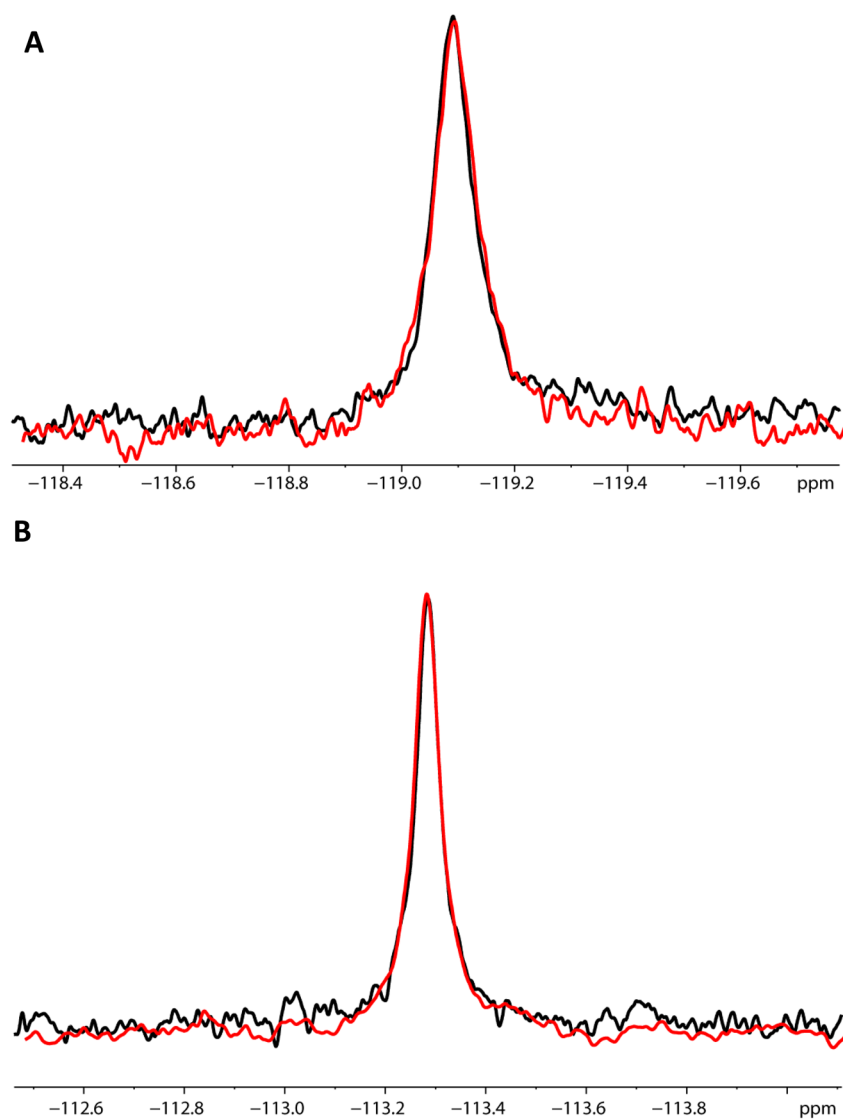


Figure 9.

Comparison of the ^{19}F spectra of flurbiprofen (**A**) and of sulindac sulfone (**B**) in the presence of bilayered lipid vesicles in the absence (black) and presence (red) of C99 (**A**) The samples contained 20 μM flurbiprofen both in the absence (black) and in the presence (red) of 100 μM C99 incorporated into 10 mM POPC/POPG vesicles (1:100 protein:vesicles). (**B**) The samples contained 20 μM sulindac sulfone in both the absence (black) and in the presence (red) of 100 μM C99 incorporated into vesicles. All control samples (black) contained only 10 mM phospholipid. The lack of change in both sets of spectra indicates that no interaction exists between the compounds and C99.